The influence of NiFe thickness of top-electrode on exchange coupling parameters of IrMn based MTJ

T. Stobiecki[b,*], C.G. Kim[a], C.O. Kim[a], Y.K. Hu[a], M. Czapkiewicz[b], J. Kanak[b], J. Wrona[b], M. Tsunoda[c], M. Takahashi[c]

[a]*Chungnam National University, Department of Materials Engineering, Daejon, 305-764, Korea*

[b]*AGH University of Science and Technology, Department of Electronics, 30-059 Krakow, Poland*

[c]*Tohoku University, Department of Electronic Engineering, Sendai 980-8579, Japan*

Elsevier use only: Received date here; revised date here; accepted date here

Abstract

MTJ's consisting of Ta(5)/Cu(10)/Ta(5)/NiFe(2)/Cu(5)/IrMn(10)/CoFe(2.5)/Al-O/CoFe(2.5)/**NiFe(t)**/Ta(5), where **t** = 10, 30, 60 and 100 nm in as-deposited and annealed state were characterized by XRD measurements: in grazing incidence (GID scan-2θ) and θ-2θ geometry, by rocking curve (scan-ω) and pole figures. The improvement of [111] texture and increase of average crystallite size of $IrMn_3$ and $Ni_{80}Fe_{20}$ layers after annealing in 300°C lead to enhancement of interfacial coupling as well interlayer coupling.

Keywords: magnetic tunneling junctions; XRD; interfacial magnetic properties;
PACS: 75.70.Cn; 61.10.-i; 61.10.Kw;

Recent works on $IrMn_3$ based MTJ's have been focused mainly on enhancement of TMR ratio, by modifying the preparation conditions of a tunnel barrier [1], or local electrical properties [2]. In this work particular attention has been paid to the correlation between structure and magnetic parameters of interfacial and interlayer exchange coupling in as deposited and annealed junctions with the structure of Ta(5)/Cu(10)/Ta(5)/NiFe(2)/Cu(5)/IrMn(10)/CoFe(2.5)/Al-O/CoFe(2.5)/**NiFe(t)**/Ta(5), where **t** = 10, 30, 60 and 100 nm. MTJ's were prepared on thermally oxidized Si wafers using DC magnetron sputtering with ultra clean Ar(9N) as the process gas, in a chamber with base pressure of 4×10^{-9} hPa. The samples were annealed in vacuum (10^{-6} hPa) at 300°C for 1 hour under a magnetic field of 80 kA/m, followed by field cooling. These are optimum annealing conditions to obtain maximum of MR ratio [3]. The magnetic measurements were performed by R-VSM and MOKE described elsewhere [4]. In order to find the correlation between structure and magnetic properties the samples have been characterized by XRD experiment (with Cu-anode) in GID (scan-2θ) and θ-2θ geometry and by rocking curve (scan-ω). Figure 1 shows the scans of θ-2θ and GID for the as-deposited and annealed stacking structures where fcc peaks of (111)$IrMn_3$, (111)Cu and (111)$Ni_{80}Fe_{20}$ are observed. Due to very close lattice planes of (111)Cu and (111)NiFe only GID measurement (under ω = 5°) allowed the separation of Cu and NiFe peaks. The pole figures of $IrMn_3$ and Cu for as-deposited and annealed samples (Fig.2) represent centered [111] spots and spread rings around angle ψ = 70°. This means that the sample has a (111) plane texture with no crystallographic orientation in the film plane. Narrow and high intensity rings for annealed samples were observed (Fig.2c, d). The annealing treatment induces an increase in (111) peak intensity, crystallites size and decrease of lattice constants and FWHM of the (111)$IrMn_3$

* Corresponding author. Tel.: +48-12-617-2596; fax: +48-12-617-3550; e-mail: stobieck@uci.agh.edu.pl.

and (111)Cu-rocking curve (see Tab.1), indicating an improvement in texture of the multilayer structure. Using high purity powder standard for calibration and program *Line Profile Analysis (LPA)* the crystallite size of (111)$IrMn_3$ (Tab.1), and (111)$Ni_{80}Fe_{20}$ (Tab.2) were determined.

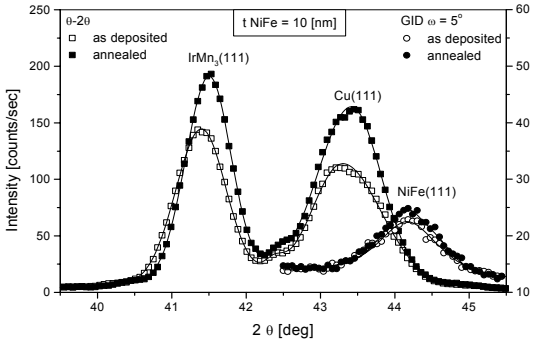

Fig.1. θ-2θ and 2θ-GID scans for as-deposited and annealed MTJ (t = 10 nm) with fitting lines of fcc-(111)$IrMn_3$, (111)Cu and (111)NiFe peaks.

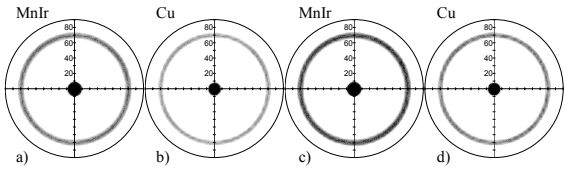

Fig.2. Pole figures of MTJ (NiFe 10 nm) for as-deposited: (a) $IrMn_3${111}, (b) Cu{111}; and annealed: (c) $IrMn_3${111} (d) Cu{111}.

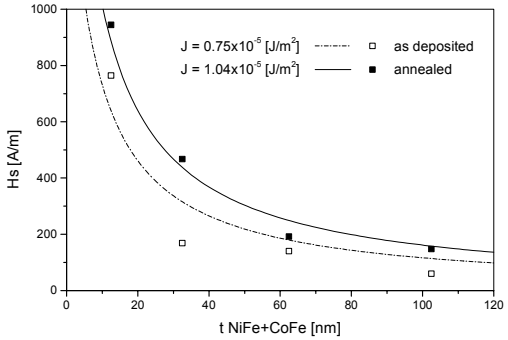

Fig.3. Free layer thickness dependence for as-deposited and annealed MTJ of the shifting field. The solid and dotted lines are fits.

Accompanied by the increase of grain size of $IrMn_3$, an increase in exchange biased field (H_{ex}) and coercivity (H_{cp}) of pinned layer $Co_{70}Fe_{30}$ was observed (Tab.1). Maximum value of H_{ex} = 110 kA/m corresponds to the interfacial exchange biased energy $J_{ex} = 47 \cdot 10^{-5}$ J/m^2. The minor loop of M(H) is always shifted in the direction indicating a ferromagnetic coupling between pinned (CoFe) and free (CoFe+NiFe) layers. The decrease of shifting field ($H_s \sim 1/t_f$) and coercivity (H_{cf}) of the free layer with increasing NiFe thickness in as-deposited and annealed samples were observed (Fig.3 and Tab.2). After annealing the interlayer coupling energy increases from $J = 0.75 \cdot 10^{-5}$ J/m^2 to $1.04 \cdot 10^{-5}$ J/m^2 whereas H_{cf} of free layer decreases. The variations of H_{cf} and H_s correlate with the size of NiFe grains (Tab.2) determined from GID measurements. The enhancement of interlayer coupling between pinned and free layers indicates the correlated in-phase roughness of magnetostatic interacting interfaces [5], due to increase of crystallites size.

In conclusion, accurately carried out XRD measurements indicate improvement of [111] texture and increased crystallites size of $IrMn_3$ after 300°C annealing, which leads to large H_{ex}. The enhancement of interlayer coupling energy is due to increase of permalloy grain size which improves magnetostatic coupling of interacting interfaces.

Table 1. Structure and magnetic parameters of $IrMn_3$, where t, a, D are given in nm, H_{ex} and H_{cp} in kA/m and FWHM in angle degree.

	as-deposited			annealed				
t	a	D	FWHM	a	D	FWHM	H_{ex}	H_{cp}
10	0.3776	7.0	5.19	0.3767	8.7	4.71	110	65
30	0.3772	7.5	5.04	0.3769	7.9	4.78	93	45
60	0.3771	7.7	4.95	0.3768	8.3	4.59	98	51
100	0.3774	7.1	5.13	0.3771	7.7	4.86	87	41

Table 2. Structure and magnetic parameters of NiFe, where H_s and H_{cf} are given in A/m.

	as-deposited				annealed			
t	a	D	H_s	H_{cf}	a	D	H_s	H_{cf}
10	0.3553	7.8	760	943	0.3553	10.1	935	764
30	0.3552	10.5	168	527	0.3548	14.3	465	282
60	0.3549	11.4	139	397	0.3547	31.7	192	177
100	0.3548	14.3	60	306	0.3545	41.7	149	243

References

[1] M. Tsunoda, K. Nishigawa, S. Ogata and M. Takahashi, Appl. Phys. Lett. 80 (2002) 3135.
[2] Y. Ando, M. Hayashi, M. Kamijo, H. Kubota, T. Miyazaki, J. Magn. Magn. Mat. 226-230 (2001) 924.
[3] Y. Saito, M. Amano, K. Nakajima, S. Takahashi, M. Sagoi, J. Magn. Magn. Mat. 223 (2001) 293.
[4] J. Wrona, T. Stobiecki, M. Czapkiewicz, R. Rak, T. Ślęzak, J. Korecki and C. G. Kim, this Conference.
[5] J.C.S. Kools, W. Kula, D. Mauri, T. Lin, J. Appl. Phys. 85 (1999) 4466.